Data Supplement

Abbreviations:
HD, healthy donors
pre, CF patients before therapy
M1, CF patients after 1 month of therapy
M6, CF patients after and 6 months of therapy

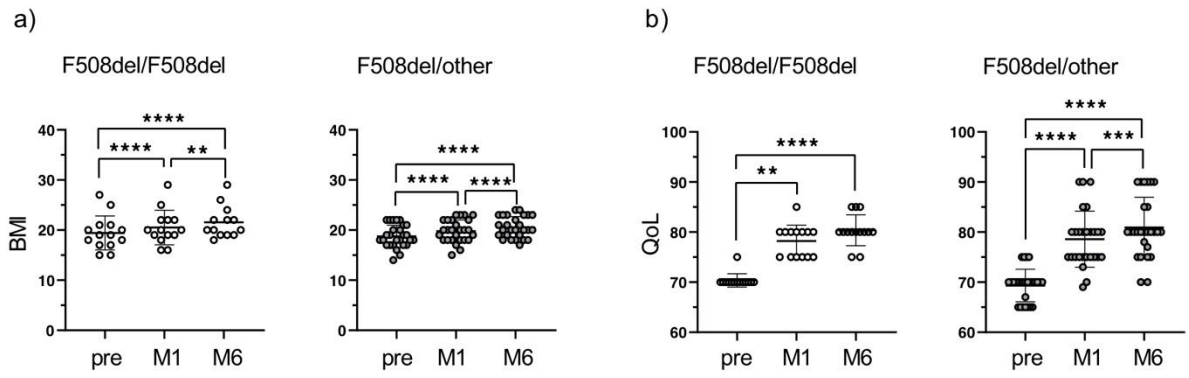

Figure S1. Improvement of body mass index (BMI) and quality of life (QoL) in patients treated with ETI. BMI and QoL in CF patients pre, M1 and M6. a) BMI of F508del/F508del (pre and M1, n=14; M6, n=13) and F508del/other (n=27). The mixed effect-model (REML) with Tukey's multiple comparison (left) and the one-way ANOVA with Tukey's multiple comparison (right) were used. b) QoL of F508del/F508del (n=14) and F508del/other (n=27). The one-way ANOVA with Tukey's multiple comparison was used. Scattered dot plot, with mean ± SEM; *, $p<0.05$; **, 0.01; ***, $p<0.001$; ****, $p<0.0001$.

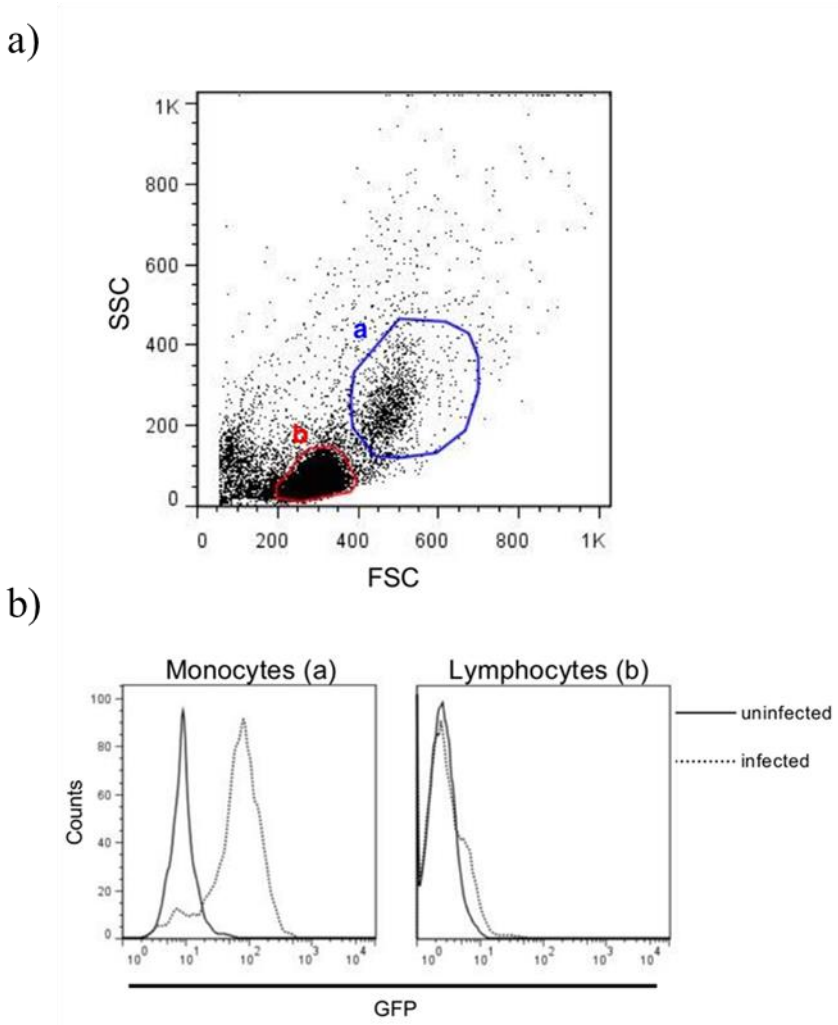

Figure S2. *P. aeruginosa* is phagocytosed only by monocytes. HD PBMCs were infected with PAO1-GFP and the phagocytosis was evaluated by flow cytometry. a) Gate strategies to identify PBMCs populations: monocytes (gate a) and lymphocytes (gate b). b) Overlaid histograms of infected monocytes (gate a) and lymphocytes (gate b). Heavy line, uninfected controls; dotted line, infected cells.

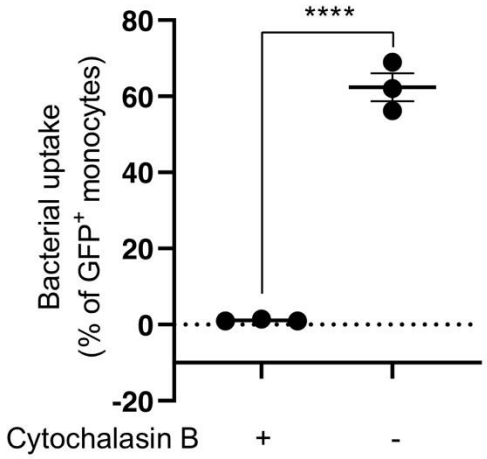

Figure S3. Cytochalasin B treatment inhibits phagocytic activity of monocytes. HD PBMCs, pretreated or not with Cytochalasin B, were infected with PAO1-GFP and phagocytosis was evaluated by flow cytometry. Scattered dot plot with mean ± SEM. Student's t-tests was used; ****, p<0,0001.

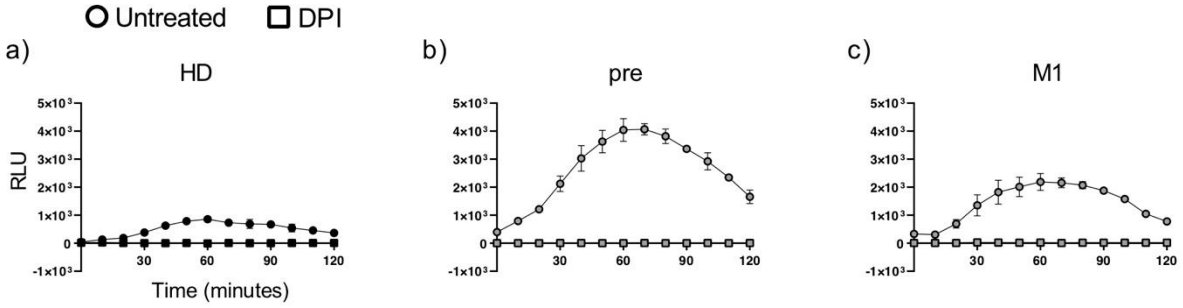

Figure S4. Diphenyleneiodonium (DPI) treatment inhibits NOX2-dependent ROS production. Samples: PBMC from HD (a) and CF pre (b) and M1 (c), pretreated (squares) or not (circles) with DPI. ROS production, following PAO1 infection, was detected every 10 min and reported as relative light unit (RLU). Data are mean ± SD of three technical replicates.

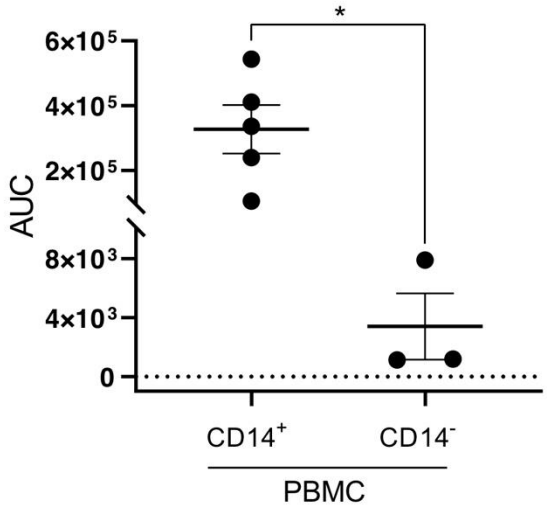

Figure S5. O_2^- production by infected HD PBMC depleted of $CD14^+$ cells. Samples: PAO1-infected PBMC ($CD14^+$) and PAO1-infected PBMC depleted of $CD14^+$ cells ($CD14^-$). O_2^- production was measured every 10 min and quantified from kinetic curves as area under the curve (AUC). The Mann-Whitney test was used. Scattered dot plot with mean ± SEM; *, $p<0.05$.

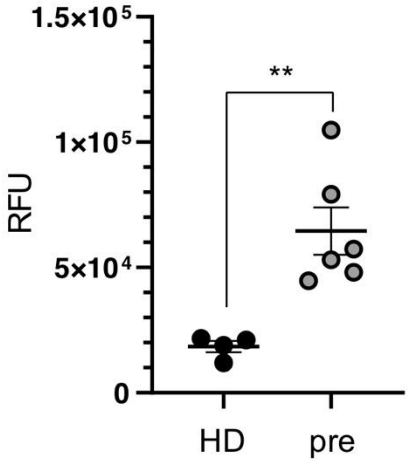

Figure S6. ROS production as detected by the H2DCFDA probe. Samples: PBMCs from HD and CF pre. Cells were infected with PAO1 and the resulting oxidative burst was measured 60 min after infection. Total ROS production is reported as relative fluorescent unit (RFU). The Student's t-test was used. Scattered dot plot with mean ± SEM; **, $p<0.01$.

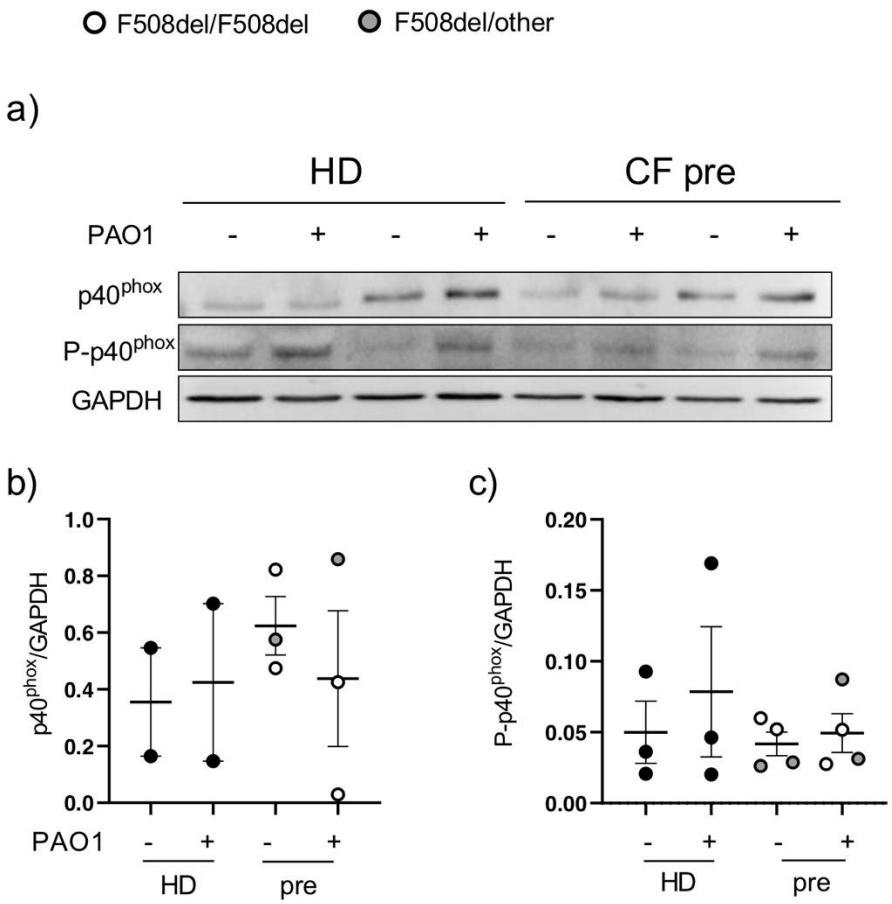

Figure S7. p40^{phox} and P-p40^{phox} in HD and CF monocytes. a) Representative WBs of two HD and two CF pre. b and c) Quantitative analysis of p40^{phox} and P-p40^{phox} respect to the loading control, GAPDH. The Brown-Forsythe ANOVA test with t-test for multiple comparison was used without detection of statistical significance among samples. Scattered dot plot with mean ± SEM.

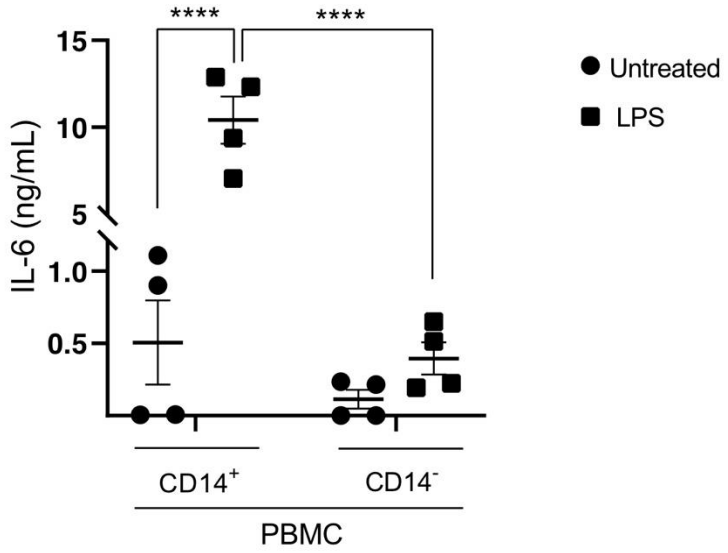

Figure S8. CD14$^+$ cells depletion abolishes IL-6 production by LPS-challenged PBMC. HD PBMC depleted (CD14-) or not depleted (CD14+) remained untreated or were stimulated with LPS. IL-6 secretion in supernatants was measured by ELISA. The two-way ANOVA test with Bonferroni multiple comparison was used. Scatter dot plot with mean ± SEM; ****, p<0.0001.

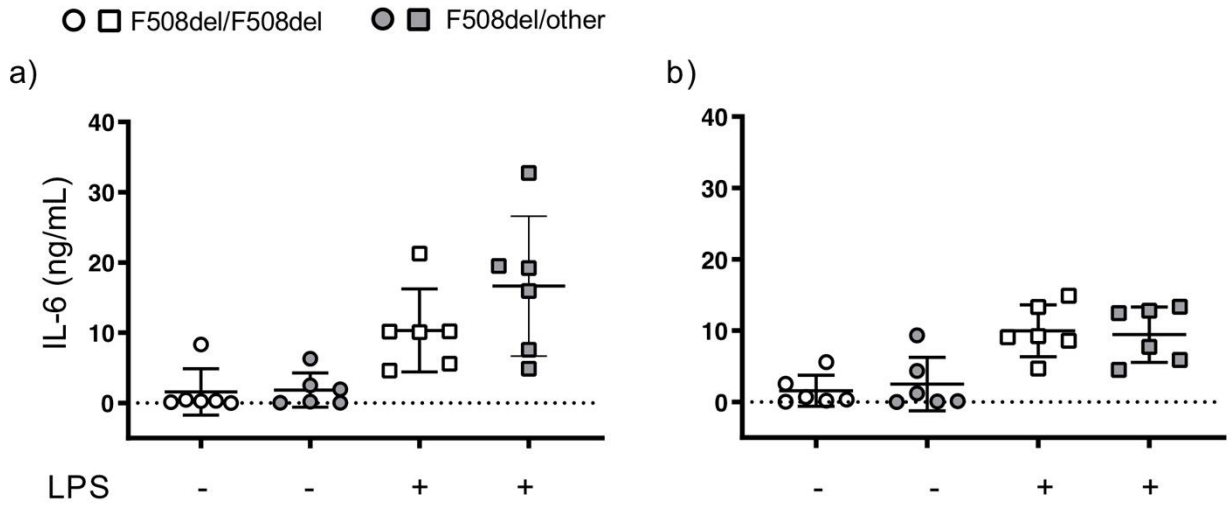

Figure S9. IL-6 production by homozygous and heterozygous patients. IL-6 secretion in supernatants of PBMCs from CF pre (a) and M1 (b). Kruskal-Wallis with Dunn multiple comparison test was used. Differences between homozygous and heterozygous subjects were not significant. Scatter dot plot with mean ± SEM.

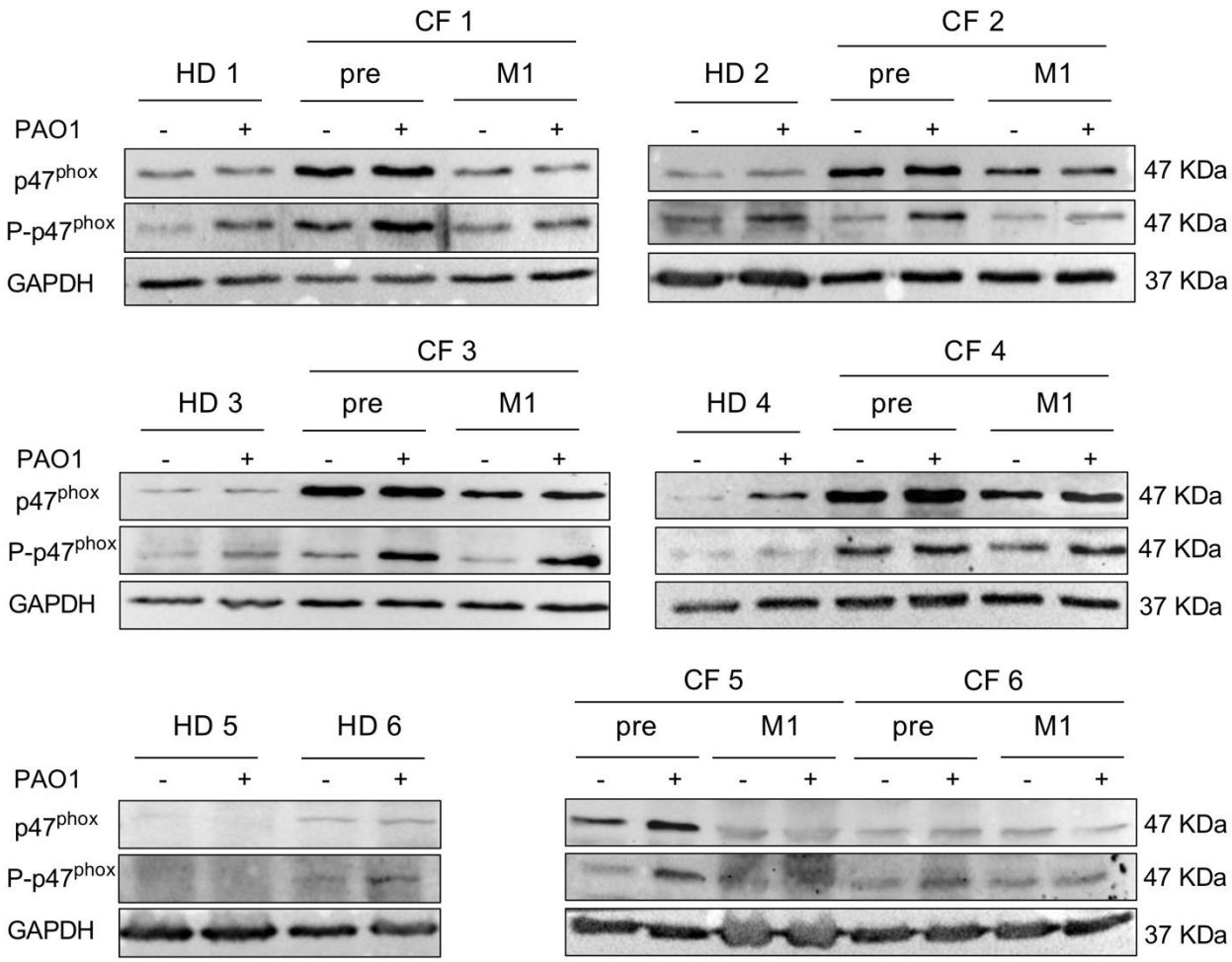

Figure S10. All blots examined for the analysis of p47^{phox} and P-p47^{phox}

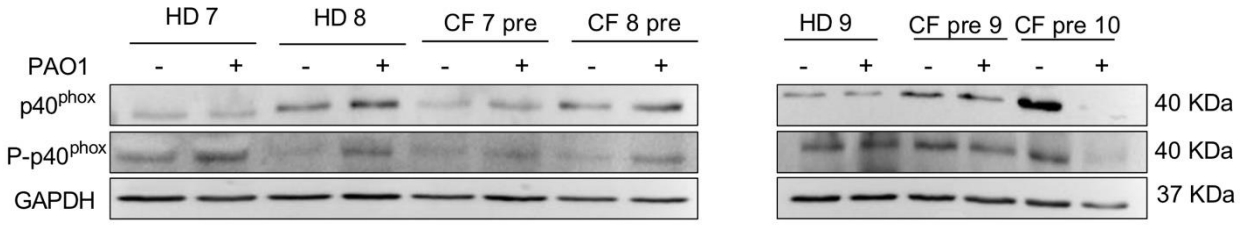

Figure S11. All blots examined for the analysis of p40^{phox} and P-p40^{phox}

Supplementary materials and methods

Table S1. Reagents, Suppliers and Identification Code (ID)

Reagent	**Suppliers**	**ID**
Anti-human Phospho-p47^{phox} (ser345) (WB, diluted 1/500)	Invitrogen	PA537806
Anti-human p47^{phox} (WB, diluted 1/500)	Santa Cruz	sc-17845
Anti-human p40^{phox} (WB, diluted 1/500)	Santa Cruz	sc-48388
Anti-human Phospho-p40^{phox} (thr154) (WB, diluted 1/1000)	Cell Signaling	#4311
Anti-GAPDH	Santa Cruz	sc-47724
Anti-human CD14	Immunotools	21620146
Anti-mouse Control IgG	Immunotools	21815016
Anti-mouse IgG	GE Healthcare	NA931V
Anti-rabbit IgG	GE Healthcare	NA934V
EasySep monocyte enrichment kit without CD16 depletion, EasySep™	StemCell	#19058
CD14 MicroBeads human	Miltenyi	130-050201
IL-6 Elisa kit	R&D	DY008
P. aeruginosa LPS	Sigma	L8643
diphenyleneiodonium (DPI)	Sigma-Aldrich	D2926
Luminol	Sigma-Aldrich	123072
2',7'-dichlorodihydrofluorescein diacetate (H2DCFDA)	Thermo Fisher Scientific	D399
Lympholyte	CEDERLANE	CL5020
RPMI with glutamine	Corning	10-040-CV
Fetal Bovine Serum (FBS)	Euroclone	ECS0180l
Premium FBS (low endotoxin)	Corning	35-015
Penicillin-Streptomycin	Corning	30-002-CI
LB Broth	Sigma	L3022
Agar	Sigma	A1296
Amikacin	Sigma	A1774
Ceftazidime	Sigma	C3809
Gentamycin	Sigma	G3632
HBSS w/o Calcium, Magnesium, Sodium Bicarbonate, Phenol Red	Euroclone	ECM0507L
Dulbecco's Phosphate Buffered Saline (DPBS) w/o Calcium Chloride, Magnesium Chloride	Sigma	D8537
BSA	Sigma	A4503
Tween®20	Sigma	P7949
Nonfat dried milk powder	ITW Reagents	A0830

Table S2. Characteristics of patients with cystic fibrosis at initiation of ETI therapy examined in supplementary figure 4, S6, S7 and S11

	F508del/F508del	***F508del/other***
N of patients	2	7
Sex, Female	2 (100%)	3 (42,8%)
Age, year	24 (±19.8)	31,57 (±13.1)
pp FEV1	70.5 (±12.02)	85.14 (±28.65)
SSC (mmol/L)	82.5 (±4.95)	90.86 (±27.11)
BMI (Kg/m^2)	17.5 (±3.53)	22.86 (±4.18)
QoL	72,5 (±3.53)	77.29 (±10.08)
	Lung Microbiology	
P. aeruginosa	1 (50%)	5 (71,4%)
S. aureus		2 (28,5%)

Data are reported as number, %, or mean ± standard deviation. Abbreviations: $ppFEV_1$, percent-predicted FEV_1; SSC, sweat chloride concentration; BMI, body mass index. Lung microbiology, the number and the percentage of patients with the indicated pathogen I reported.

Table S3. Percentage of GFP^+ monocytes in PAO1-GFP infected PBMC from CF pre, M1 and M6

pre	M1	M6
79,5	67,7	51
70	62,35	53,07
65,2	60,6	73,45↑
64,4	**82↑**	**69,54↑**
61,9	**73,15↑**	**70,66↑**
55,9	66,35↑	40,1
52	60↑	46,1
51,58	**70,5↑**	**58,79↑**
48,9	nd	40
47,8	**80↑**	**76↑**
45,4	**62,1↑**	**74,9↑**
41,5	nd	45↑
38	**37**	**54,5↑**
37,14	52,68↑	61,31↑
35,6	nd	nd
32,2	56,4↑	60,2↑
12,94	40,95↑	35,07↑
5,3	nd	76,6↑
nd	nd	63,9
nd	nd	59,75
nd	73,9	nd

Each row refers to one subject; data from CF F508del/F508del samples are reported in bold; ↑subjects showing a percent increase of the GFP^+ monocyte respect to pre; nd, not determined.

Table S4. Killing activity of PAO1-infected PBMC from CF pre, M1 and M6

pre	M1	M6
-126,42	**35,11**	**28,31**
-11,11	**44,58**	**19,63**
-7,69	30,01	17,24
-5,44	**32,51**	-0,36
-3,86	19,63	38,90
-3,70	**47,74**	**40,84**
-3,52	**25,49**	-0,61
-2,59	nd	-3,34
-0,21	**21,75**	**48,86**
1,99	nd	nd
2,91	**34,36**	**44,10**
8,52	41,42	37,65

Percentage reduction of viable bacteria recovered from PBMC infected with PAO1 as obtained by the intracellular killing assay. Negative results indicate intracellular bacterial growth rather than killing. Each row refers to one subject; homozygous F508del/F508del samples are reported in bold; nd, not determined.

Detailed methods

Bacteria. *P. aeruginosa* strains: laboratory strain PAO1; clonal clinical strains isolated from the same patient at the beginning of lung infection, AA2, and at the end of the lung disease, AA44; they are considered as representative of the early and late CF isolates, respectively (1). PAO1 was transformed with pUC30T-*gfpmut*3 plasmid (PAO1-GFP) and cultured in LB medium supplemented with 50 µg/mL gentamycin; the clinical isolates AA2 and AA44 were cultured in antibiotic-free LB medium. Cultures from frozen stocks were grown over night at 37°C with shaking (180 rpm), refreshed 1/10 in pre-warmed LB medium and grown to exponential phase (OD_{600}≈ 0,5). Bacteria were washed with PBS, resuspended in antibiotic-free cell-culture medium and used to infect PBMC samples at a MOI of 20.

PBMC isolation. Peripheral blood was collected by venipuncture into EDTA-vacutainers. PBMCs were isolated by density gradient centrifugation, collected, and washed three times with PBS supplemented with FBS 2% and EDTA 1mM. Subsequently, the cells were washed with PBS and resuspended in antibiotic-free RPMI supplemented with FBS 20% (10^6/mL) and used based on the experimental protocols. PBMC were depleted of $CD14^+$ cells using anti-CD14 mAb coupled to

magnetic beads followed by immunomagnetic selection (Miltenyi Biotec, Bergisch Gladbach, Germany). The depletion, evaluated by staining with an anti-CD14 monoclonal antibody, was ≥ 90%.

Flow Cytometry. PBMCs were washed twice with PBS and incubated with conjugated human monoclonal anti-CD14 or isotype control antibodies in the dark for 20 min on ice. After incubation, cells were washed and freshly analyzed. The analysis was performed as follow: i) forward and side scatter plots; ii) monocytes based on FSC-SSC were gated; iii) percentages of positivity to anti-CD14 antibody. The range of events analyzed was 10.000-100.000. CellQuest and FlowJo softwares were used for sample collection and data analysis, respectively.

Phagocytosis Assay by Flow Cytometry. PBMCs ($5x10^5$) were infected with PAO1-GFP at a MOI of 20 for 30 min. at 37°C in 5% CO_2. When applied, cells were pre-treated with 10 µM Cytochalasin B for 30 min. At the end of infection, PBMCs were gently washed twice with PBS and analyzed by flow cytometry as described above. Phagocytosis was evaluated as the percentage of GFP^+ events calculated on the non-infected cutoff. Additionally, to evaluate the possible phagocytosis activity of PBMC cells other than monocytes, GFP positivity was also evaluated in the other PBMC populations.

PBMCs Infection and Analysis of Bacterial Uptake and Intracellular Killing. $5x10^5$ of freshly isolated PBMCs were infected with *P. aeruginosa* strains. When applied, PBMCs were pretreated with DPI (10 µM, for 30 min at 37°C in 5% CO_2). Infection was synchronized by centrifugation and the infected cells were then incubated at 37°C in 5% CO_2 for 30 min. At the end of the infection, cells were treated with antibiotics (amikacin and ceftazidime, 1 mg/mL each) at 37°C for 15 min, to eliminate non-phagocytosed bacteria. Afterwards, the infected cells were washed twice and recovered in PBS for the analysis of bacterial uptake or in culture medium to evaluate the microbicidal activity. For the latter, cells were incubated for 60 min at 37°C and 5%CO2 in culture medium supplemented with sub-inhibitory concentration of antibiotics (0.1 mg/mL each). CFUs at the end of infection (t_0) and one hour after infection (t_{60}) were determined by plating aliquots in LB plates.

Bactericidal activity was calculated as follows: (CFU_{t0} – CFU_{t60}) / CFU_{t0} x 100.
Additionally, bacterial killing of PBMC was calculated with linear regression model to determine the slope values of killing curves.

ROS Measurement. Luminol probe was used to measure intracellular O_2^- levels as described in Cavinato *et al*., 2020 (2) with minor modifications. Briefly, PBMC, pretreated or not with DPI (10 µM, for 30 min at 37°C in 5% CO_2) were resuspended in HBSS without phenol red supplemented with luminol, 25µg/mL. $5x10^5$ cells/well were seeded in white 96-well plates and infected with *P. aeruginosa* at a MOI of 20. The chemiluminescence was measured every 10 min up to 120 min with the multilabel counter CLARIOstar PLUS (BMG LABTECH). The data were corrected based on the controls without PBMC. Quantitative analysis of O_2^- production was performed by determination of the area under the curve (AUC) using the GraphPad Prism software.
ROS measurement by the H2DCFDA probe was performed according to the supplier's specification. Briefly, PBMC ($5x10^5$) were resuspended in HBSS without phenol red, seeded in black 96-well plate and infected with *P. aeruginosa* for 30 min 37°C in 5% CO_2. Subsequently, cells were load with H2DCFDA (10 µM) probe for further 30 min and gently washed with HBSS without phenol red. Fluorescence was measured (excitation 495/absorption 525 nm) with the multilabel counter. DPI-treated controls were included. Data were corrected on the uninfected controls.

Western Blots. Monocytes were isolated by negative selection using EasySep monocyte enrichment kit without CD16 depletion, following the manufacturer's specifications. Collected cells were incubated in complete culture medium without antibiotics and infected with PAO1 at a MOI=20 for 30 min at 37°C in 5% CO2. Non-infected controls were also included. After infection, cells were treated with antibiotics, gently washed twice and finally lysed in HEPES 50 mM, NaCl 150 mM, EGTA 10 mM, NP-140 1%, NaF 100 mM, Na3VO4 8 mM, Glycerol 5%, Pefabloc 2 mM, proteinase cocktail inhibitor. Western Blots were performed with 30 µg of proteins according to Mecocci *et al*., 2020 (3). Membranes were blocked with 5% skimmed milk, in PBS-Tween 20 (0,1%) or 5% BSA in TBS-Tween 20 (0,1%) and stained with primary and secondary antibodies (Supplementary Table 1).

Cytokine quantification. Cytokine quantification was performed as previously reported (4) in supernatants of monocytes untreated or treated for 18 hr with *P. aeruginosa* LPS, 500 ng/ml, in culture medium supplemented with low endotoxin FBS 2%.

Supplementary References

1. Cigana C, Curcurù L, Leone MR, Ieranò T, Lorè NI, Bianconi I, Silipo A, Cozzolino F, Lanzetta R, Molinaro A, Bernardini ML, Bragonzi A. Pseudomonas aeruginosa exploits lipid A and muropeptides modification as a strategy to lower innate immunity during cystic fibrosis lung infection. *PLoS One*. 2009;4:12.
2. Cavinato L, Genise E, Luly FR, Di Domenico EG, Del Porto P, Ascenzioni F. Escaping the Phagocytic Oxidative Burst: The Role of SODB in the Survival of Pseudomonas aeruginosa Within Macrophages. *Front Microbiol* 2020;11:326.
3. Mecocci S, Gevi F, Pietrucci D, Cavinato L, Luly FR, Pascucci L, Petrini S, Ascenzioni F, Zolla L, Chillemi G, Cappelli K. Anti-Inflammatory Potential of Cow, Donkey and Goat Milk Extracellular Vesicles as Revealed by Metabolomic Profile. *Nutrients* 2020;12.
4. Luly FR, Lévêque M, Licursi V, Cimino G, Martin-Chouly C, Théret N, Negri R, Cavinato L, Ascenzioni F, Del Porto P. MiR-146a is over-expressed and controls IL-6 production in cystic fibrosis macrophages. *Sci Rep* 2019;9:16259.